Available online at www.sciencedirect.com

SciVerse ScienceDirect

Taiwanese Journal of Obstetrics & Gynecology 50 (2011) 474–478

www.tjog-online.com

Short Communication

Non-classical estrogen receptors action on human dermal fibroblasts

Kuan-Hao Tsui [a,1], Peng-Hui Wang [b,c,1], Chia-Kai Chen [d], Yi-Jen Chen [b,c], Shih-Hwa Chiou [e,f], Yen-Jen Sung [d,**], Hsin-Yang Li [b,c,d,*]

[a] *Department of Obstetrics and Gynecology, Kaohsiung Veterans General Hospital, Kaohsiung, Taiwan*
[b] *Department of Obstetrics and Gynecology, Taipei Veterans General Hospital, Taipei, Taiwan*
[c] *Department of Obstetrics and Gynecology, Faculty of Medicine, School of Medicine, National Yang-Ming University, Taipei, Taiwan*
[d] *Institute of Anatomy and Cell Biology, School of Medicine, National Yang-Ming University, Taipei, Taiwan*
[e] *Institute of Pharmacology, School of Medicine, National Yang-Ming University, Taipei, Taiwan*
[f] *Department of Education and Research, Taipei Veterans General Hospital, Taipei, Taiwan*

Accepted 13 September 2011

Abstract

Objective: To study the possible non-genomic effect of selective estrogen receptor modulators on human dermal fibroblasts (HDF).
Materials and Methods: WS1 cells were used to test the effect of raloxifene. The mRNA expressions of estrogen receptor (ER) α and β and G protein-coupled ER 1(GRP30) were examined by reverse transcription polymerase chain reaction. Apoptosis was identified by TUNEL assay and FACS analysis. MAPK and PI3 K/Akt pathways were determined by immunoblotting analysis.
Results: Neither ERα nor ERβ, but GPR30 was detected in WS1 cells. Raloxifene increased apoptosis, which was blocked by pertussis toxin, an inhibitor of G protein, or by LY294002. Phosphorylated p38 MAPK and Akt were also increased after raloxifene treatment.
Conclusion: SERMs could induce apoptosis of HDF through G protein and PI3 K/Akt signaling, which may help understand the role of SERMs on the skin.

Keywords: Apoptosis; Estrogen; Human dermal fibroblasts; Non-genomic; Selective estrogen receptor modulator

Introduction

A number of studies have shown the important roles of estrogen on the skin, based on the changes that are seen in postmenopausal women [1]. However, despite the knowledge that estrogens have such important effects on skin and estrogen receptors (ERs) have been detected in the skin, the cellular and subcellular sites and mechanisms of estrogen action are still poorly understood [2]. In addition, there is very limited data available addressing the effects of selective estrogen receptor modulators (SERMs) on skin [2]. Due to the potential risk of the use of estrogen after menopausal status, SERMs have been considered as a possible alternative in postmenopausal women [3–6]. Classically, estrogen action is mediated through ER dimers, including ERα and ERβ [7, 8]. However, non-genomic or ER-independent estrogen action is shown. Therefore, it is reasonable to suppose that these molecules, such as SERMs, might act on the skin through a non-genomic effect. An orphan receptor G protein-coupled estrogen receptor 1 (GPR30), which belongs to one of several guanine nucleotide-binding protein (G-protein)-coupled receptors [9, 10], is also reported to be one of the estrogen-mediated non-genomic effects.

The aim of this study was to determine the possible non-genomic effect of estrogen, and SERMs on skin; therefore,

* Corresponding author. Department of Obstetrics and Gynecology, Taipei Veterans General Hospital, 201 Shih-Pai Road Section 2, Taipei 112, Taiwan.
** Corresponding author. Institute of Anatomy and Cell Biology, School of Medicine, National Yang-Ming University, 155 Li-Nong Street Section 2, Taipei 112, Taiwan.
E-mail addresses: yjsung@ym.edu.tw (Y.-J. Sung), lihy@vghtpe.gov.tw (H.-Y. Li).
[1] These authors contributed equally to this work.

1028-4559/$ - see front matter
doi:10.1016/j.tjog.2011.10.013

WS1 cells, human dermal fibroblasts (HDFs) without expression of both ERα and ERβ, were tested.

Materials and methods (Supplementary materials and methods)

Reagents

Reagents for the treatment of HDF were prepared as follows: raloxifene (RAL), G protein inhibitor pertussis toxin (from Sigma, St Louis, MO, USA), PI3 K inhibitor LY294002, ERK inhibitors PD98059, and p38 MAPK inhibitor SB203580 (from Calbiochem; San Diego, CA, USA) were dissolved in dimethylsulfoxide (DMSO; Sigma).

Cell culture

The normal human fetal skin fibroblast cell line, WS1, was isolated from the midscapular skin of a 12-week-old African-American female embryo; this line has a doubling potential of 67. The cells were cultured in minimum essential medium (MEM; Gibco, Grand Island, NY, USA) supplemented with 10% fetal bovine serum (FBS; Hyclone, Logan, UT, USA), 2 mM L-glutamine (Sigma), 100 units/mL penicillin (Sigma), and 100 μg/mL streptomycin (Sigma). Cells were maintained in 100-mm tissue culture dishes in a humidified chamber at 5% CO_2 and 37°C, and subcultured every 2 to 3 days by trypsin-EDTA (Gibco, Grand Island, NY, USA). For all subsequent experiments, WS1 cells were seeded in MEM Alpha medium without phenol red (α-MEM without phenol red; Gibco). After 18 hours of incubation, the medium was replaced and the cells were subjected to various drug treatments.

WST1 assay

WST1 cell proliferation reagent (Roche, Mannheim, Germany) measures the metabolic activity of viable cells. Cells were seeded in 96-well plates at 5×10^3 cells/100 μL/well. Following 18 hours of incubation, various drugs were added to the cell culture. After the indicated time, the supernatants were discarded and the cells were washed with phosphate buffered saline (PBS). Then, WST1 was added to each well at a 1:20 dilution, and the cells were incubated at 37°C for a further 2 hours. The supernatants were quantified spectrophotometrically at 450 nm, with a reference wavelength at 640 nm. Data were presented as the percentage of survival relative to that in a vehicle-treated control culture. All WST1 assays were performed in duplicate.

RNA isolation and RT-PCR

Total RNA was collected with the RNeasy kit (Qiagen, Milan, Italy) as described by the manufacturer. For reverse transcription polymerase chain reaction (RT-PCR) studies, first-strand cDNA was synthesized from 1–5 μg of total RNA with an oligo(dT) primer and Super Script II reverse transcriptase (Invitrogen, Life Technologies, Inc., Carlsbad, CA, USA). Primers for human ERα, ERβ, GPR30, and GAPDH genes are as follows (5′ to 3′): ERα, forward, CTA CTG CAT CAG ATC CAA GG; reverse, GTC ATT GGT ACT GGC CAA TCT; ERβ, forward, TGG TCA GGG ACA TCA TCA TGG; reverse, TCA AAG AGG GAT GCT CAC TTC TG; GPR30, forward, GGC TTT GTG GGC AAC ATC; reverse, CGG AAA GAC TGC TTG CAG G; GADPH, forward, ATT GTT GCC ATC AAT GAC CC; reverse, AGT AGA GGC AGG GAT GAT GT. The conditions used for amplification were as follows: 94°C for 30 seconds followed by 52°C for 1 minute and 72°C for 30 seconds in a 25-μL reaction buffer containing cDNA generated from 1 μL of cDNA, 0.2 mM of each dNTP, 0.2 μM of each primer, and 2.5 units of *Taq* polymerase. Detection of the amount of PCR product after 35 cycles was performed after electrophoresis on 1.5% agarose gels and ethidium bromide staining.

Detection of apoptosis by TUNEL analysis

Apoptosis of the single cell is detected by fluorescent labeling of DNA strand breaks (a hallmark of apoptosis). Cells were plated in 35-mm culture dishes at 5×10^5 per dish and cultured overnight, followed by the administration of test reagents. After an indicated interval of drug treatments, the supernatant was discarded and the cells were collected by trypsinization. The cells were washed twice with PBS and fixed by incubating in 4% paraformaldehyde at room temperature for 1 hour. After another PBS wash, the cells were permeabilized by resuspension in 0.1% Triton X-100 (Sigma) in 0.1% sodium citrate (Sigma) on ice for 2 minutes, followed by a PBS wash. Then a 50 ml TUNEL reaction mixture (*In Situ* Cell Death Detection Kit; Roche), which contained terminal deoxynucleotidyl transferase and fluorescein-labeled nucleotides, was added and the cells were incubated at 37°C for 1 hour in the dark. After a further PBS wash, the cells were subjected to fluorescence-activated cell scanning analysis (FACS; BD, Palo Alto, CA, USA) with excitation at 488 nm and emission at 525–550 nm.

FACS analysis for activated caspases in apoptotic cells

CaspACE FITC-VAD-FMK in situ marker (Promega, Madison, WI, USA) is a fluoroisothiocyanate (FITC) conjugate of the cell-permeable caspase inhibitor VAD-FMK. This structure allows delivery of the inhibitor into the cell, where it binds to activated caspases, serving as an in situ marker for apoptosis. Cells cultured in 35-mm dishes were treated with various drugs. At the end of cell culture, the supernatant was removed and the cells were detached by trypsin-EDTA. After two consecutive PBS washes, the cells were stained with 10 μM CaspACE FITC-VAD-FMK *In Situ* Marker, followed by incubation at room temperature in the dark for 20 minutes. Cells were then washed with PBS and subjected to FACS analysis with excitation at 488 nm and emission at 525–550 nm.

Immunoblotting assay

Immunoblotting assays were performed to measure the synthesis of procollagen type I and to detect the activation of

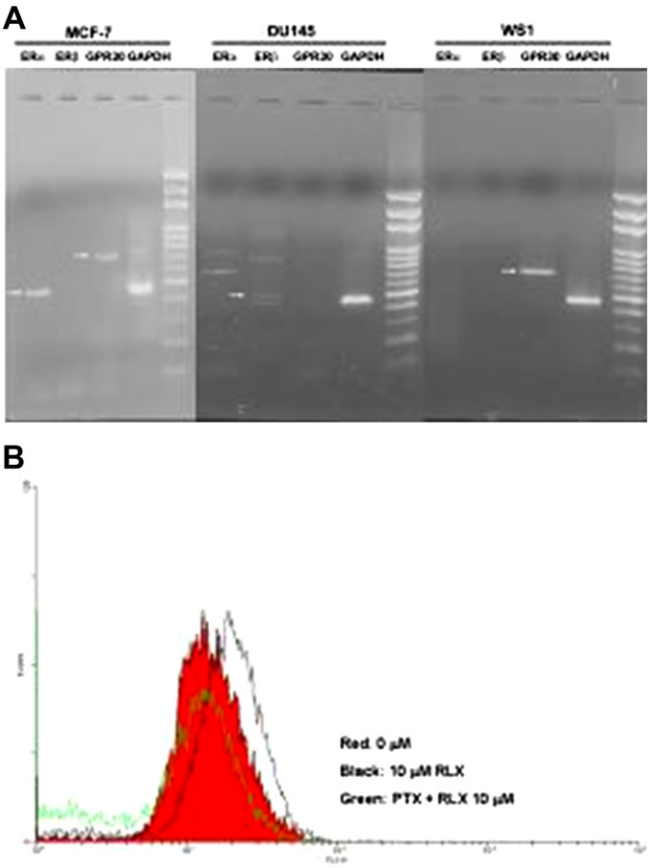

Fig. 1. (A) Detection of mRNA expression of ERα, ERβ, and GPR30 in WS1 cells by RT-PCR; (B) WS1 cells were pretreated with or without 0.25 μg/mL pertussis toxin (PTX) 1 hour before the addition of 10 μM RAL or the corresponding vehicle, followed by culture for 24 hours. Subsequently, TUNEL staining and FACS analysis were performed.

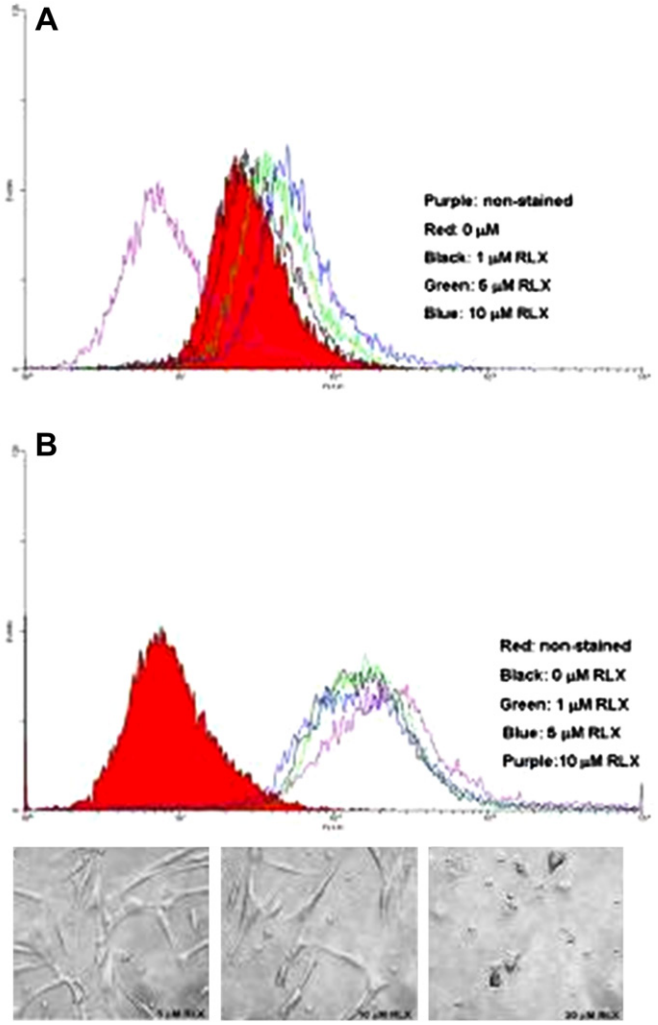

Fig. 2. (A) Detection of apoptosis by TUNEL staining; (B) measurement of activated caspases by VAD-FMK staining in WS1 cells treated with RAL.

MAPKs and Akt. Cells were plated in 35-mm culture dishes at 5×10^5 per dish and cultured overnight, followed by the addition of various drugs. The treatments were terminated after indicated intervals by aspirating supernatants and washing the dishes with PBS. The cells were lysed by keeping the dish on ice for 5 minutes with 70 μL of lysis buffer (20 mM Tris, pH 7.5, 150 mM NaCl, 1 mM EDTA, 1 mM EGTA, 1% Triton, 2.5 mM sodium pyrophosphate, 1 mM β-glycerophosphate, 1 mM Na_3VO_4, 1 μg/mL leupeptin, and 1 mM phenylmethylsulfonyl fluoride). The lysed cells were scraped off the dish, transferred to microcentrifuge tubes, and vortexed for 10 seconds. The cell lysates were then centrifuged at 18000 × *g*, 4°C for 10 minutes to remove insoluble material, and the protein concentration of each sample was measured. Approximately 15–50 μg of supernatant protein from each sample was fractionated by 10% SDS-polyacrylamide gel electrophoresis. After electrophoresis, the fractionated cellular proteins were transferred to polyvinylidene fluoride membranes (PVDF; NEN Life Science Products, Inc., Boston, MA, USA). For immunoblotting, the membranes were blocked with 5% non-fat milk in TBST [25 mM Tris, pH 7.5, 150 mM NaCl, 0.1% (v/v) Tween 20] and incubated overnight at 4°C with one of the following primary antibodies: rabbit anti-human phospho-ERK antibody, rabbit anti-human ERK antibody, rabbit anti-human phospho-JNK antibody, rabbit anti-human JNK antibody, rabbit anti-human phospho-p38 antibody, rabbit anti-human p38 antibody (Cell Signaling Technology, Beverly, MA, USA), goat anti-human procollagen type I antibodies (Santa Cruz Technology, Santa Cruz, CA, USA), or mouse anti-human actin antibody (Upstate Technology, Charlottesville, VA, USA). The PVDF membranes were then extensively washed with TBST and incubated for 60 minutes at room temperature with corresponding secondary antibodies: goat anti-rabbit antibody, donkey anti-goat antibody (Santa Cruz Technology), or goat anti-mouse antibody (Upstate Technology). After extensive washing with TBST, the immune complexes were detected by chemiluminescence using the Western Blotting analysis system (NEN Life Science Products, Inc., Boston, MA, USA).

Statistical analysis

Data of the WST1 assays were analyzed by analysis of variance (ANOVA), followed by Fisher's *post-hoc* least significant difference (LSD) test. A p value <0.05 was

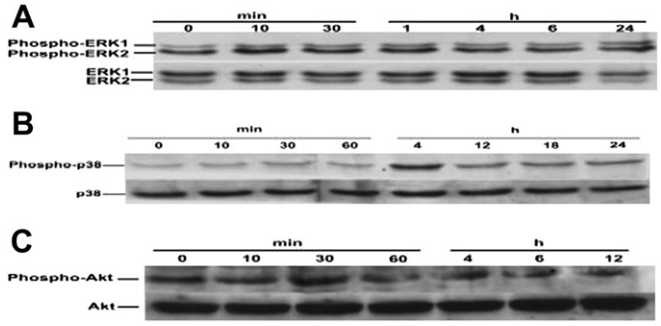

Fig. 3. Effects of RAL on: (A) phospho-ERK1 and ERK2; (B) phospho-p38; and (C) phospho-Akt activation in WS1 cells.

designated as statistically significant. All analyses were performed using the SAS program (SAS Institute Inc., Cary. NC, USA).

Results

Confirmation of absent expression of ERα and ERβ but presence of GPR30 on WS1 cells

We used MCF7 breast cancer and DU145 prostate cancer cells for positive controls of ERα and ERβ. There was neither ERα nor ERβ mRNA expression in the WS1 cells. By contrast, GPR30 mRNA was detected in the WS1 cells (Fig. 1A). Following the above results, we supposed that the apoptosis of WS1 induced by raloxifene may be mediated by GPR30. To test this hypothesis, we added 0.25 μm/mL pertussis toxin (PTX), an inhibitor of G protein signaling, 1 hour before the administration of RAL, followed by TUNEL staining and flow cytometry. The RAL-induced apoptosis was significantly inhibited by pre-treatment with PTX (Fig. 1B).

Apoptosis of WS1 was increased by RAL treatment

We used TUNEL staining and FACS analysis for detection of DNA strand breaks to assess whether WS1 cell death caused by RAL was due to apoptosis. After treatment with 1−10 μM RAL for 24 hours, all cells were collected, stained, and analyzed by flow cytometry. We found that RAL could increase the percentage of TUNEL-positive cells in a dose-dependent manner (Fig. 2A). On the other hand, RAL was found to increase the level of fluorescent staining with activated caspases only at 10 μM (Fig. 2B).

Apoptosis was mediated by ERK, MAPK and Akt pathways in WS1 cells treated with RAL

To study which signal transduction pathway (ERK, MAPK or Akt) was involved in RAL-induced apoptosis, WS1 cells were treated with 10 μM RAL, followed by protein extraction for immunoblotting analysis. The level of phosphorylated ERK (phospho-ERK1 and ERK2) was not increased upon exposure to RAL (Fig. 3A). Phosphorylated p38 MAPK (phosphor-p38) significantly increased under RAL treatment after 4 hours (Fig. 3B). Akt, the downstream target of PI3 K, was activated at 30 minutes after stimulation with RAL (Fig. 3C). Then, we used an inhibitor (SB203580, PD98059, LY294002) to inhibit the above signal transduction pathway. Inhibition of PI3 K/Akt with LY294002 successfully rescued cells from RAL-induced apoptosis (Fig. 4).

Discussion

Deterioration of the skin with age in women may result from many factors, including genetic and environmental factors [11]. Among these, estrogen might be one of the

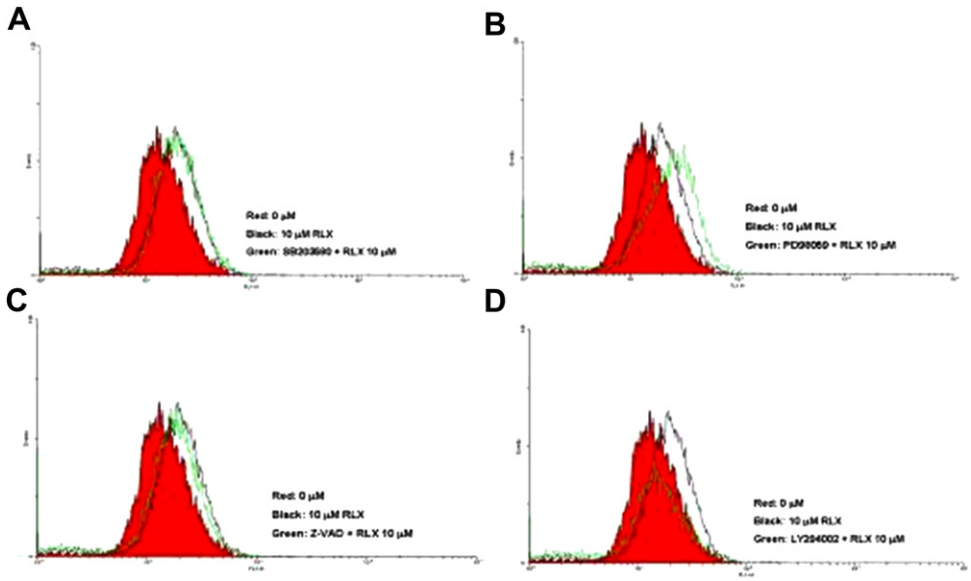

Fig. 4. Effects of p38 MAPK, ERK and PI3 K inhibitors on RAL-induced apoptosis. WS1 cells were pre-treated with: (A) 20 μM SB203580 (a p38 MAPK inhibitor); (B) 20 μM PD98059 (an ERK inhibitor); (C) 50 μM Z-VAD (a caspase inhibitor); and (D) 20 μM LY294002 (a PI3 K inhibitor) 1 hour before the administration of 10 μM RAL. Cell culture was continued for 24 hours. Then, TUNEL staining was performed and detected by FACS analysis.

important factors, because declining estrogen levels are associated with a variety of skin changes in women, and the expression of cutaneous ERs is also decreased after the menopause [12]. However, in addition to estrogen, SERMs were also reported to be capable of interaction with ERs, though with a different affinity to the subtypes of ERs [13]. However, a recent study showed the possibility of a non-genomic effect of estrogen or SERMs, including identification of a rapid non-genomic effect of E_2 on intracellular Ca2+ ([Ca2+]i) signaling in the eccrine sweat gland epithelial cell line NCL-SG3 [14]. To study the possibility of the non-genomic effect of SERMs on skin tissue, an ER-negative HDF cell line, WS1, was used to test our hypothesis.

In this study, SERMs showed a strong inhibition of the cell growth of these ER-negative cells. TUNEL staining and FACS analysis showed apoptosis of these cells was significant at high concentrations (above 1 μM) with the use of RAL, suggesting that the toxic effect of the SERMs might not be mediated through the classical ER pathway.

In clarifying the above hypothesis, RT-PCR analysis verified that WS1 cells were positive for GPR30 mRNA expression [9, 10]. We used pertussis toxin (PTX), which could disrupt G protein signaling, in the management of WS1 cells before the administration of SERMs, and found that the SERM-inducing apoptosis of WS1 cells could be blocked, suggesting that the GPR pathway was involved in the apoptosis of WS1 cells after SERM treatment. Furthermore, we identified the p38 MAPK and PI3 K/Akt pathway in WS1 cells treated with RAL and found activation of the p38 MAPK and PI3 K/Akt pathway, suggesting that this pathway might also involve the apoptosis of WS1 cells. To confirm this hypothesis, we used an inhibitor, the LY294002 of PI3 K/Akt pathway, in the management of WS1 cells treated with RAL, and successfully rescued these cells from RAL-induced apoptosis. The results demonstrated that RAL could induce apoptosis in HDF via G protein signaling and the PI3 K/Akt pathway. In an updated study, G protein-coupled estrogen receptor (GPER) expressed in the cardiovascular system, has recently been identified. Endogenous human 17β-estradiol, SERMs including tamoxifen and raloxifene, and selective estrogen receptor downregulators, such as ICI182780, are all agonists of GPER, which has been implicated in the regulation of vasomotor tone and protection from myocardial ischemia/reperfusion injury [15]. The possible signal transduction pathway of RAL on WS1 cells is depicted in Fig. 5.

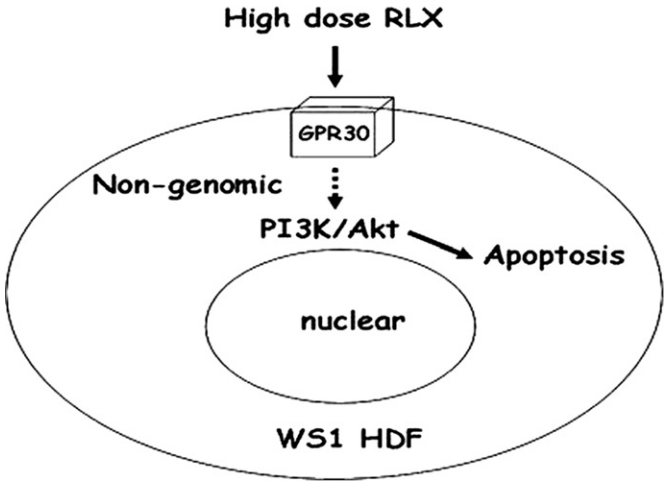

Fig. 5. A proposed model of signaling pathways of RLX-induced apoptosis in HDF. High-dose RLX could bind to membrane-bound GPR30 and then activate PI3 K/Akt to induce apoptosis in HDF, which belongs to the non-genomic pathway.

Conclusions

Our results established that RAL could induce apoptosis via the G protein and PI3 K/Akt pathways in WS1 cells.

References

[1] Stevenson S, Thornton J. Effect of estrogens on skin aging and the potential roles of SERMs. Clin Interv Aging 2007;2:283–97.
[2] Verdier-Sévrain S, Bonté F, Gilchrest B. Biology of estrogens in skin: implications for skin aging. Exp Dermatol 2006;15:83–94.
[3] Wang PH, Chao HT. Reconsideration of tamoxifen use for breast cancer. Taiwan J Obstet Gynecol 2007;46:93–5.
[4] Lee WL, Cheng MH, Chao HT, Wang PH. The role of selective estrogen receptor modulator on breast cancer-from tamoxifen to raloxifene. Taiwan J Obstet Gynecol 2008;47:24–31.
[5] Wang PH, Chao HT. To switch or not to switch: should the study of tamoxifen and raloxifene (STAR) trial alter our decision? Taiwan J Obstet Gynecol 2008;47:372–4.
[6] Lee WL, Chao HT, Cheng MH, Wang PH. Rationale for using raloxifene to prevent both osteoporosis and breast cancer in postmenopausal women. Maturitas 2008;60:92–107.
[7] Wang YN, Wu W, Chen HC, Fang H. Genistein protects against UVB-induced senescence-like characteristics in human dermal fibroblast by p66Shc down-regulation. J Dermatol Sci 2010;58:19–27.
[8] Couse JF, Korach KS. Estrogen receptor null mice: what have we learned and where will they lead us? Endocr Rev 1999;20:358–417.
[9] Quinn JA, Graeber CT, Frackelton Jr AR, Kim M, Schwarzbauer JE, Filardo EJ. Coordinate regulation of estrogen-mediated fibronectin matrix assembly and epidermal growth factor receptor transactivation by the G protein-coupled receptor, GPR30. Mol Endocrinol 2009;23:1052–64.
[10] Filardo EJ, Thomas P. GPR30: a seven-transmembrane-spanning estrogen receptor that triggers EGF release. Trends Endocrinol Metab 2005;16:362–7.
[11] Phillips TJ, Symons J, Menon S. HT study group. Does hormone therapy improve age-related skin changes in postmenopausal women? A randomized, double-blind, double-dummy, placebo-controlled multicenter study assessing the effects of norethindrone acetate and ethinyl estradiol in the improvement of mild to moderate age-related skin changes in postmenopausal women. J Am Acad Dermatol 2008;59:397–404.e3.
[12] Kuiper GG, Carlsson B, Grandien K, Ennask E, Haggblad J, Nilsson S, et al. Comparison of the ligand binding specificity and transcript tissue distribution of estrogen receptor α and β. Endocrinology 1997;138:863–70.
[13] Marini H, Polito F, Altavilla D, Irrera N, Minutoli L, Calò M, et al. Genistein aglycone improves skin repair in an incisional model of wound healing: a comparison with raloxifene and oestradiol in ovariectomized rats. Br J Pharmacol 2010;160:1185–94.
[14] Muchekehu RW, Harvey BJ. 17beta-estradiol rapidly mobilizes intracellular calcium from ryanodine-receptor-gated stores via a PKC-PKA-Erk-dependent pathway in the human eccrine sweat gland cell line NCL-SG3. Cell Calcium 2008;44:276–88.
[15] Matthias RM, Eric RP, Matthias B. The G protein-coupled estrogen receptor GPER/GPR30 as a regulator of cardiovascular function. Vascular Pharmacology 2011;55:17–25.